nature

https://doi.org/10.1038/s41586-021-03471-w

Accelerated Article Preview

Escape of SARS-CoV-2 501Y.V2 from neutralization by convalescent plasma

Received: 21 January 2021

Accepted: 18 March 2021

Accelerated Article Preview Published online 29 March 2021

Cite this article as: Cele, S. et al. Escape of SARS-CoV-2 501Y.V2 from neutralization by convalescent plasma. *Nature* https://doi.org/10.1038/s41586-021-03471-w (2021).

Sandile Cele, Inbal Gazy, Laurelle Jackson, Shi-Hsia Hwa, Houriiyah Tegally, Gila Lustig, Jennifer Giandhari, Sureshnee Pillay, Eduan Wilkinson, Yeshnee Naidoo, Farina Karim, Yashica Ganga, Khadija Khan, Mallory Bernstein, Alejandro B. Balazs, Bernadett I. Gosnell, Willem Hanekom, Mahomed-Yunus S. Moosa, NGS-SA, COMMIT-KZN Team, Richard J. Lessells, Tulio de Oliveira & Alex Sigal

Article

Escape of SARS-CoV-2 501Y.V2 from neutralization by convalescent plasma

https://doi.org/10.1038/s41586-021-03471-w

Received: 21 January 2021

Accepted: 18 March 2021

Published online: 29 March 2021

Sandile Cele[1,2], Inbal Gazy[2,3,4], Laurelle Jackson[1], Shi-Hsia Hwa[1,5], Houriiyah Tegally[3], Gila Lustig[6], Jennifer Giandhari[3], Sureshnee Pillay[3], Eduan Wilkinson[3], Yeshnee Naidoo[3], Farina Karim[1,2], Yashica Ganga[1], Khadija Khan[1], Mallory Bernstein[1], Alejandro B. Balazs[7], Bernadett I. Gosnell[8], Willem Hanekom[1,5], Mahomed-Yunus S. Moosa[8], NGS-SA*, COMMIT-KZN Team*, Richard J. Lessells[2,3,6], Tulio de Oliveira[2,3,6,9] ✉ & Alex Sigal[1,2,10] ✉

SARS-CoV-2 variants of concern (VOC) have arisen independently at multiple locations [1, 2] and may reduce the efficacy of current vaccines targeting the spike glycoprotein [3]. Here, using a live virus neutralization assay (LVNA), we compared neutralization of a non-VOC variant versus the 501Y.V2 variant using plasma collected from adults hospitalized with COVID-19 from two South African infection waves, with the second wave dominated by 501Y.V2 infections. Sequencing demonstrated that infections in first wave plasma donors were with viruses harbouring none of the 501Y.V2-defining mutations, except for one with the E484K mutation in the receptor binding domain. 501Y.V2 virus was effectively neutralized by plasma from second wave infections and first wave virus was effectively neutralized by first wave plasma. In cross-neutralization, 501Y.V2 virus was poorly neutralized by first wave plasma, with a 15.1-fold drop relative to 501Y.V2 neutralization by second wave plasma across participants. In contrast, second wave plasma cross-neutralization of first wave virus was more effective, showing only a 2.3-fold decline relative to first wave plasma neutralization of first wave virus. While we only tested one plasma elicited by E484K alone, this potently neutralized both variants. The observed effective neutralization of first wave virus by 501Y.V2 infection elicited plasma provides preliminary evidence that vaccines based on VOC sequences could retain activity against other circulating SARS-CoV-2 lineages.

Through genomic surveillance of the severe acute respiratory syndrome-related coronavirus 2 (SARS-CoV-2), a number of new variants have been identified with multiple mutations in the spike glycoprotein. We recently described the emergence of the 501Y.V2 (B.1.351) variant in South Africa, characterized by the K417N, E484K, and N501Y mutations in the spike receptor binding domain (RBD) as well as four substitutions and a deletion in the N-terminal domain (NTD).[1,2] This variant was first detected in October 2020, and has rapidly become the dominant variant in South Africa with a frequency in January 2021 of 97% according to the GISAID (https://www.gisaid.org/hcov19-mutation-dashboard/).

The RBD is the main target of neutralizing antibodies (NAbs) elicited by SARS-CoV-2 infection, with the remaining activity directed at the NTD.[4,5] All three amino acid residues in the RBD that carry mutations in 501Y.V2 interact directly with the human angiotensin-converting enzyme 2 (hACE2) receptor and form part of the epitopes for hACE2-blocking NAbs.[6] The E484 residue specifically is a hotspot for binding of highly potent NAbs.[6] In a number of separate *in vitro* studies using monoclonal antibodies (mAbs), mutations at E484 have emerged as immune escape mutations, often conferring broad cross-resistance to panels of mAbs.[7–10] E484K also emerged during passage with convalescent plasma, leading to substantial drops in neutralization.[11,12] Using a deep mutation scanning approach to determine the effect of individual mutations on neutralization by polyclonal sera, mutations at E484 were associated with the largest drops in neutralization.[13]

South Africa experienced two SARS-CoV-2 infection waves to date (https://coronavirus.jhu.edu/map.html). The first wave peaked in July 2020 and consisted of viral variants which usually showed the D614G mutation but none of the defining mutations of 501Y.V2. These variants have been almost completely supplanted by 501Y.V2 variants in the second South African infection wave, peaking January 2021.

Coinciding with our initial report, there have been multiple studies showing that 501Y.V2 decreases neutralization capacity of polyclonal antibodies elicited by non-501Y.V2 SARS-CoV-2 infection or vaccination. The decrease ranges from relatively moderate[14–17] to severe.[18–23] Importantly, three clinical trials performed in South Africa during the second, 501Y.V2 infection wave reported dramatic decreases in vaccine efficacy. The Novavax NVX-CoV2373 subunit vaccine demonstrated

[1]Africa Health Research Institute, Durban, 4001, South Africa. [2]School of Laboratory Medicine and Medical Sciences, University of KwaZulu-Natal, Durban, 4001, South Africa. [3]KwaZulu-Natal Research Innovation and Sequencing Platform, Durban, 4001, South Africa. [4]Department of Biochemistry and Molecular Biology, The Institute for Medical Research Israel-Canada, Hadassah Medical School, The Hebrew University of Jerusalem, 91120, Jerusalem, Israel. [5]Division of Infection and Immunity, University College London, London, WC1E 6BT, UK. [6]Centre for the AIDS Programme of Research in South Africa, Durban, 4001, South Africa. [7]Ragon Institute of MGH, Harvard, and MIT, Cambridge, USA. [8]Department of Infectious Diseases, Nelson R. Mandela School of Clinical Medicine, University of KwaZulu-Natal, Durban, 4001, South Africa. [9]Department of Global Health, University of Washington, Seattle, USA. [10]Max Planck Institute for Infection Biology, Berlin, 10117, Germany. *Lists of authors and their affiliations appear in the Supplementary Information. ✉e-mail: deoliveira@ukzn.ac.za; alex.sigal@ahri.org

a decrease in efficacy from 89.3% to 49.4% (https://ir.novavax.com/news-releases/news-release-details/novavax-covid-19-vaccine-demonstrates-893-efficacy-uk-phase-3). This trial also reported no difference in infection frequency between SARS-CoV-2 seropositive and seronegative participants in the placebo arm, indicating that infection with non-501Y.V2 virus does not protect against 501Y.V2 re-infection. Details of the seroprevalence testing are not yet available. The Johnson and Johnson adenovirus vectored single dose vaccine showed a reduced efficacy from 72% in the US to 57% in South Africa. (https://www.jnj.com/johnson-johnson-announces-single-shot-janssen-covid-19-vaccine-candidate-met-primary-endpoints-in-interim-analysis-of-its-phase-3-ensemble-trial). Most strikingly, the AstraZeneca ChAdOx1 AZD1222 chimpanzee adenoviral vectored vaccine showed only 10% efficacy against 501Y.V2 variants, compared to 75% efficacy against earlier South African variants.[3] The roll-out of this vaccine in South Africa is currently paused.

Here, using a live virus neutralization assay (LVNA), we measured the degree to which 501Y.V2 virus compromises neutralization elicited by natural infection with non-501Y.V2 variants. We also measure the degree to which the earlier variants could escape the neutralizing response elicited to 501Y.V2 virus (Figure 1a). We used plasma samples from our ongoing longitudinal cohort that tracks COVID-19 cases enrolled at hospitals in Durban, South Africa.[24] We sampled participants weekly for the first month post-enrollment. At each timepoint a blood draw and combined nasopharyngeal/oropharyngeal swab was performed to obtain both the plasma and infecting virus. Swabs positive for SARS-CoV-2 were sequenced.

We chose plasma from 14 participants from the first South African infection wave where the infecting virus was successfully sequenced (Materials and Methods). Plasma samples were from blood drawn approximately 1 month post-symptom onset (Extended Data Table 1), close to the antibody response peak.[25] Of the 14 participants, 13 did not show RBD or NTD mutations in the infecting virus. A single participant sampled in October 2020 showed the E484K escape mutation in the absence of the other 501Y.V2 mutations (Supplementary Table 1). We had fewer participants from the second infection wave at the time of writing as most have not yet reached the 1 month post-symptom onset time-point for sampling. The second wave participants in this study were infected late December 2020 or early January 2021 (Figure 1b, Extended Data Table 1). We were able to sequence three second wave participants where sequence allowed variant calling, two of which had good spike coverage (Figure 1b, Supplementary Table 1). In all cases, the infecting variant was 501Y.V2. It is extremely likely that 501Y.V2 was also the infecting variant for the rest of the participants from infection wave 2, given the complete dominance of this variant in January 2021. For each second wave participant, our clinical team conducted a telephonic interview and examined clinical records to determine if the participant was also infected in the first South African infection wave. None of the participants showed evidence of being previously infected.

We outgrew first wave virus (Materials and Methods) from one participant during the first infection wave, and second wave, 501Y.V2 virus from a sample obtained in November 2020 through our genomic surveillance program (Figure 1b). We used a microneutralization live virus focus forming assay[26] which relies on a methylcellulose overlay to limit cell-free viral spread, resulting in a local infection focus. The focus is detected by an anti-SARS-CoV-2 spike antibody (Materials and Methods). We normalized the number of foci to the number of foci in the absence of plasma on the same plate to obtain the transmission index (Tx,[27]). This controls for experimental variability in the input virus dose between experiments. We mixed the virus with serially diluted plasma, then added the mixture to Vero E6 cells and counted infection foci after 28 hours using automated image analysis (Extended Data Figure 1A, Figure 2a, Materials and Methods).

There was a clear reduction in neutralization capacity of 501Y.V2 by first wave plasma relative to neutralization of the homologous, first wave variant (Extended Data Figure 1). 501Y.V2 also showed larger foci, likely reflecting a larger number of cells infected by one infected cell, or more rapid infection cycles (Figure 2a, Extended Data Figure 1A). In order to compare foci of similar size we reduced the incubation time of 501Y.V2 infection to 18 hours. In order to detect some effect of first wave plasma on the 501Y.V2 variant, we tested more concentrated plasma (Figure 2a, b). To rule out infection saturation effects, we obtained a positive control monoclonal antibody with similar neutralization of first wave and 501Y.V2 variants. We then repeated the experiments (Extended Data Figures 2–4 show representative neutralization experiments for each participant plasma).

We observed the same trend in neutralization capacity as with the first set of experiments: there was a decline in the number of foci when first wave plasma was added to the homologous, first wave virus. This was strongly attenuated with 501Y.V2 (Figure 2b). When second wave, 501Y.V2 elicited plasma was used, it effectively neutralized the homologous, 501Y.V2 variant (Figure 2c). In contrast to the first wave plasma, substantial cross-neutralization of first wave virus was observed. Some of the foci were smaller at higher antibody concentrations (Figure 2c, Extended Data Figures 2–4), possibly indicative of some reduction in cell-to-cell spread by neutralizing antibodies in the Vero E6 cell line.

The data from the focus forming assay at each dilution approximated a normal distribution (Extended Data Figure 5) and we therefore used parametric statistics to describe it. We fitted the data for each participant to a sigmoidal function[28] with the dilution required to inhibit 50% of infection (ID_{50}) as the only free parameter (Materials and Methods). For clarity, we plotted the data for each neutralization experiment as percent neutralization ($(1-Tx)\times 100\%$, Materials and Methods,[18]), with neutralization represented by the 50% plaque reduction neutralization titer ($PRNT_{50}$,[17]), the reciprocal of the ID_{50}.

The Genscript BS-R2B2 rabbit monoclonal neutralizing antibody (NAb, referred to by its catalog number, A02051) was used as a positive control in each experiment (Extended Data Figures 2–4). This antibody showed a similar neutralization response between variants (Figure 2d) and was used to test that that focus number/size was not saturating per experiment. We also used a plasma pool from 3 study participants who did not have any indications of SARS-CoV-2 infection, and this plasma pool did not appreciably neutralize either variant (Figure 2d).

We then proceeded to quantify neutralization of the homologous virus and cross-neutralization. First wave virus infection was neutralized by first wave plasma, with some variability in neutralization capacity between first wave infected participants. It was also cross-neutralized by second wave, 501Y.V2 elicited plasma (Figure 2d). There was overlap between neutralization capacity of first wave and second wave plasma. In contrast, when the 510Y.V2 variant was used as the infecting virus, there was a clear separation between the neutralization capacity of the homologous second wave (Figure 2d) versus the heterologous first wave plasma. While the homologous plasma effectively neutralized 501Y.V2, the cross-neutralization mediated by first wave plasma was weaker, consistent with what is apparent when viewing the raw number of foci (Figure 2b, c, Extended Data Figures 2–4). Plasma elicited by the variant with the E484K mutation alone showed much stronger neutralization of both the first wave and 501Y.V2 virus relative any of the other plasma samples (Figure 2d).

The $PRNT_{50}$ values showed a strong reduction in first wave plasma cross-neutralization of 501Y.V2 virus (Figure 2e). Excluding the plasma elicited by the virus with E484K mutation alone, which showed a very high $PRNT_{50}$ for both variants, first wave plasma $PRNT_{50}$ declined between 3.2 to 41.9-fold with the 501Y.V2 variant. In contrast, the decline in $PRNT_{50}$ in cross-neutralization of first wave virus by second wave 501Y.V2 elicited plasma was more attenuated. Here, the decline ranged between 1.6 to 7.2-fold relative to the homologous 501Y.V2 virus (Figure 2e).

Given the data approximated a normal distribution (Extended Data Figure 5), we derived the mean neutralization between first wave

(excluding the plasma elicited with the E484K only virus) and second wave participants (Figure 3). In both cases, neutralization showed a separation across all dilutions tested between the homologous and heterologous virus, where cross-neutralization was lower. However, the separation was less with 501Y.V2 elicited plasma cross-neutralization of first wave virus (Figure 3). To quantify homologous versus cross-neutralization capacity, we repeated the sigmoidal fit to the combined participant means and obtained the combined $PRNT_{50}$. For first wave plasma neutralization of first wave virus, $PRNT_{50}$ was 344.0 with fit 95% confidence intervals of 275.4–458.0 (Figure 3 summary table, top left blue rectangle). For second wave plasma neutralization of the homologous, 501Y.V2 virus (Figure 3 summary table, bottom right blue rectangle), $PRNT_{50}$ was 619.7 (517.8–771.5). Hence, 501Y.V2 elicited a robust antibody response in the participants tested. For cross-neutralization, first wave plasma cross-neutralization of 501Y.V2 virus (Figure 3, bottom left yellow rectangle) was strongly attenuated across participants, with $PRNT_{50}$ = 41.1 (32.7–55.5). In contrast, second wave plasma cross-neutralization of first wave virus (Figure 3, top right yellow rectangle) was more effective at $PRNT_{50}$ = 149.7 (132.1–172.8). 95% confidence intervals did not overlap between any of the conditions.

Fold-change decrease of first wave plasma neutralization of 501Y.V2 compared to homologous virus was 8.4. Fold-change decrease of second wave plasma neutralization of first wave compared to homologous virus was 4.1. However, absolute 501Y.V2 plasma neutralization capacity of first wave virus dropped only 2.3-fold compared to first wave plasma. In contrast, it decreased 15.1-fold when 501Y.V2 was cross-neutralized by first wave plasma (Figure 3).

The significance of these results is that 501Y.V2 is poorly neutralized by plasma elicited by non-501Y.V2 variants. However, 501Y.V2 infection elicited plasma not only effectively neutralized 501Y.V2 virus, but also more successfully cross-neutralized the earlier variant (Figure 2). This cross-neutralization is within the lower part of the neutralization capacity range elicited by the Pfizer BNT162b2 mRNA vaccine.[14,15,17] Due to potentially higher immunogenicity of 501Y.V2 variant indicated by the high $PRNT_{50}$ of 501Y.V2 elicited plasma, this plasma does not greatly under-perform the plasma elicited by earlier, non-501Y.V2 variants when neutralizing these earlier variants.

The larger focus size in 501Y.V2 relative to first wave virus is unlikely to influence results. We performed 501Y.V2 infections with larger foci using the same infection incubation time as first wave virus, and also 501Y.V2 infections where focus size was similar using a shorter 501Y.V2 infection incubation time. The results showed similar trends. Furthermore, neutralization by the monoclonal antibody control indicated that the system could effectively read out unsaturated neutralization for both variants (Figure 2d, Extended Data Figures 2–4). 501Y.V2 variants vary in some of their mutations. The variant we used has an L18F mutation in the NTD which currently occurs in about a quarter of 501Y.V2 variants (GISAID). Other 501Y.V2 mutation patterns require further investigation. An important question in the interpretation of the results is whether the second wave infected participants were also infected in the first infection wave. Our clinical team conducted telephonic interviews and investigated the clinical charts and found no evidence of previous SARS-CoV-2 infection. While previous infection may still be missed despite these measures, we believe it is unlikely to have occurred in all the second wave participants. Lastly, while we and others measured plasma neutralization, how well this correlates to protection at the mucosal surface where initial infection takes place is yet unclear.

The plasma elicited by virus with the E484K mutation alone showed the strongest neutralization both of the first wave and the 501Y.V2 virus relative to any of the other plasma samples tested (Figure 2). Because we only found one participant in this category, this result is difficult to interpret: it may be due to high immunogenicity of the mutant or because of participant specific factors. Our clinical data does not show prolonged SARS-CoV-2 shedding in this participant or other unusual features (Extended Data Table 1). This result highlights the importance of sequencing the infecting virus, and requires further investigation.

The recent Novavax, Johnson and Johnson, and AstraZeneca South African vaccine trial results indicate that the 501Y.V2 variant may lead to a decrease in vaccine efficacy. The loss of neutralization capacity in 501Y.V2 infection we quantified among the vaccinated participants in the AstraZeneca trial[3] shows that loss of neutralization may be associated with loss of vaccine efficacy. Loss of vaccine efficacy may also be mediated by escape from T cell immunity, although this is less likely due to the diversity of HLA alleles in the population, which may curtail the ability of an escape variant which evolved in one individual to escape T cell immunity in another.[29] If loss of vaccine efficacy proves to require vaccine redesign, the results presented here may be the first indication that a vaccine designed to target 501Y.V2 may also effectively target other SARS-CoV-2 variants.

Online content

Any methods, additional references, Nature Research reporting summaries, source data, extended data, supplementary information, acknowledgements, peer review information; details of author contributions and competing interests; and statements of data and code availability are available at https://doi.org/10.1038/s41586-021-03471-w.

1. H. Tegally, E. Wilkinson, M. Giovanetti, A. Iranzadeh, V. Fonseca, J. Giandhari, D. Doolabh, S. Pillay, E. J. San, N. Msomi, K. Mlisana, A. von Gottberg, S. Walaza, M. Allam, A. Ismail, T. Mohale, A. J. Glass, S. Engelbrecht, G. Van Zyl, W. Preiser, F. Petruccione, A. Sigal, D. Hardie, G. Marais, M. Hsiao, S. Korsman, M. A. Davies, L. Tyers, I. Mudau, D. York, C. Maslo, D. Goed212 hals, S. Abrahams, O. Laguda-Akingba, A. Alisoltani-Dehkordi, A. Godzik, C. K. Wibmer, B. T. Sewell, J. Lourenco, L. C. J. Alcantara, S. L. Kosakovsky Pond, S.Weaver, D. Martin, R. J. Lessells, J. N. Bhiman, C. Williamson, and T. de Oliveira. Emergence of a SARS-CoV-2 variant of concern with mutations in spike glycoprotein. *Nature*, 2021. ISSN 1476-4687 (Electronic) 0028-0836 (Linking). https://doi.org/10.1038/s41586-021-03402-9. URL https://www.ncbi.nlm.nih.gov/pubmed/33690265.
2. N. R. Faria, T. A. Mellan, C.Whittaker, I. M. Claro, D. D. S. Candido, S. Mishra, M. A. E. Crispim, F. C. Sales, I. Hawryluk, J. T. McCrone, R. J. G. Hulswit, L. A. M. Franco, M. S. Ramundo, J. G. de Jesus, P. S. Andrade, T. M. Coletti, G. M. Ferreira, C. A. M. Silva, E. R. Manuli, R. H. M. Pereira, P. S. Peixoto, M. U. Kraemer, N. Gaburo, C. D. C. Camilo, H. Hoeltgebaum, W. M. Souza, E. C. Rocha, L. M. de Souza, M. C. de Pinho, L. J. T. Araujo, F. S. V. Malta, A. B. de Lima, J. D. P. Silva, D. A. G. Zauli, A. C. S. Ferreira, R. P. Schnekenberg, D. J. Laydon, P. G. T. Walker, H. M. Schluter, A. L. P. Dos Santos, M. S. Vidal, V. S. Del Caro, R. M. F. Filho, H. M. Dos Santos, R. S. Aguiar, J. L. P. Modena, B. Nelson, J. A. Hay, M. Monod, X. Miscouridou, H. Coupland, R. Sonabend, M. Vollmer, A. Gandy, M. A. Suchard, T. A. Bowden, S. L. K. Pond, C. H. Wu, O. Ratmann, N. M. Ferguson, C. Dye, N. J. Loman, P. Lemey, A. Rambaut, N. A. Fraiji, Mdpss Carvalho, O. G. Pybus, S. Flaxman, S. Bhatt, and E. C. Sabino. Genomics and epidemiology of a novel sars-cov-2 lineage in manaus, brazil. *medRxiv*, 2021. https://doi.org/10.1101/2021.02.26.21252554. URL https://www.ncbi.nlm.nih.gov/pubmed/33688664.
3. Shabir A. Madhi, Vicky Baillie, Clare L. Cutland, Merryn Voysey, Anthonet L. Koen, Lee Fairlie, Sherman D. Padayachee, Keertan Dheda, Shaun L. Barnabas, Qasim Ebrahim Bhorat, Carmen Briner, Gaurav Kwatra, Khatija Ahmed, Parvinder Aley, Sutika Bhikha, Jinal N. Bhiman, As'ad Ebrahim Bhorat, Jeanine du Plessis, Aliasgar Esmail, Marisa Groenewald, Elizea Horne, Shi-Hsia Hwa, Aylin Jose, Teresa Lambe, Matt Laubscher, Mookho Malahleha, Masebole Masenya, Mduduzi Masilela, Shakeel McKenzie, Kgaogelo Molapo, Andrew Moultrie, Suzette Oelofse, Faeezah Patel, Sureshnee Pillay, Sarah Rhead, Hylton Rodel, Lindie Rossouw, Carol Taoushanis, Houriiyah Tegally, Asha Thombrayil, Samuel van Eck, Constantinos Kurt Wibmer, Nicholas M. Durham, Elizabeth J Kelly, Tonya L Villafana, Sarah Gilbert, Andrew J Pollard, Tulio de Oliveira, Penny L. Moore, Alex Sigal, and Alane Izu. Safety and e_cacy of the ChAdOx1 nCoV-19 (AZD1222) Covid-19 vaccine against the B.1.351 variant in South Africa. *medRxiv*, 2021. https://doi.org/10.1101/2021.02.10.21251247. URL https://www.medrxiv.org/content/early/2021/02/12/2021.02.10.21251247.
4. L. Piccoli, Y. J. Park, M. A. Tortorici, N. Czudnochowski, A. C. Walls, M. Beltramello, C. Silacci-Fregni, D. Pinto, L. E. Rosen, J. E. Bowen, O. J. Acton, S. Jaconi, B. Guarino, A. Minola, F. Zatta, N. Sprugasci, J. Bassi, A. Peter, A. De Marco, J. C. Nix, F. Mele, S. Jovic, B. F. Rodriguez, S. V. Gupta, F. Jin, G. Piumatti, G. Lo Presti, A. F. Pellanda, M. Biggiogero, M. Tarkowski, M. S. Pizzuto, E. Cameroni, C. Havenar-Daughton, M. Smithey, D. Hong, V. Lepori, E. Albanese, A. Ceschi, E. Bernasconi, L. Elzi, P. Ferrari, C. Garzoni, A. Riva, G. Snell, F. Sallusto, K. Fink, H. W. Virgin, A. Lanzavecchia, D. Corti, and D. Veesler. Mapping neutralizing and immunodominant sites on the SARS-CoV-2 spike receptor-binding domain by structure-guided high-resolution serology. *Cell*, **183**(4):1024–1042 e21, 2020. ISSN 1097-4172 (Electronic) 0092-8674 (Linking). https://doi.org/10.1016/j.cell.2020.09.037. URL https://www.ncbi.nlm.nih.gov/pubmed/32991844.
5. Matthew McCallum, Anna De Marco, Florian Lempp, M. Alejandra Tortorici, Dora Pinto, Alexandra C. Walls, Martina Beltramello, Alex Chen, Zhuoming Liu, Fabrizia Zatta, Samantha Zepeda, Julia di Iulio, John E. Bowen, Martin Montiel-Ruiz, Jiayi Zhou, Laura E. Rosen, Siro Bianchi, Barbara Guarino, Chiara Silacci Fregni, Rana Abdelnabi, Shi-Yan Caroline Foo, Paul W. Rothlauf, Louis-Marie Bloyet, Fabio Benigni, Elisabetta Cameroni, Johan Neyts, Agostino Riva, Gyorgy Snell, Amalio Telenti, Sean P.J. Whelan, Herbert W. Virgin,

Davide Corti, Matteo Samuele Pizzuto, and David Veesler. N-terminal domain antigenic mapping reveals a site of vulnerability for SARS-CoV-2. *bioRxiv*, page 2021.01.14.426475, 2021. https://doi.org/10.1101/2021.01.14.426475. URL https://www.biorxiv.org/content/biorxiv/early/2021/01/14/2021.01.14.426475.full.pdf.

6. C. O. Barnes, C. A. Jette, M. E. Abernathy, K. A. Dam, S. R. Esswein, H. B. Gristick, A. G. Malyutin, N. G. Sharaf, K. E. Huey-Tubman, Y. E. Lee, D. F. Robbiani, M. C. Nussenzweig, Jr. West, A. P., and P. J. Bjorkman. SARS-CoV-2 neutralizing antibody structures inform therapeutic strategies. *Nature*, **588**(7839):682–687, 2020. ISSN 1476-4687 (Electronic) 0028-0836 (Linking). https://doi.org/10.1038/s41586-020-2852-1. URL https://www.ncbi.nlm.nih.gov/pubmed/33045718.
7. Alina Baum, Benjamin O Fulton, Elzbieta Wloga, Richard Copin, Kristen E Pascal, Vincenzo Russo, Stephanie Giordano, Kathryn Lanza, Nicole Negron, and Min Ni. Antibody cocktail to SARS-CoV-2 spike protein prevents rapid mutational escape seen with individual antibodies. *Science*, **369**(6506):1014–1018, 2020. ISSN 0036-8075.
8. A. J. Greaney, T. N. Starr, P. Gilchuk, S. J. Zost, E. Binshtein, A. N. Loes, S. K. Hilton, J. Huddleston, R. Eguia, K. H. D. Crawford, A. S. Dingens, R. S. Nargi, R. E. Sutton, N. Suryadevara, P. W. Rothlauf, Z. Liu, S. P. J. Whelan, R. H. Carnahan, Jr. Crowe, J. E., and J. D. Bloom. Complete mapping of mutations to the SARS-CoV-2 spike receptor-binding domain that escape antibody recognition. *Cell Host Microbe*, 2020. ISSN 1934-6069 (Electronic) 1931-3128 (Linking). https://doi.org/10.1016/j.chom.2020.11.007. URL https://www.ncbi.nlm.nih.gov/pubmed/33259788.
9. Z. Liu, H. Zheng, H. Lin, M. Li, R. Yuan, J. Peng, Q. Xiong, J. Sun, B. Li, J. Wu, L. Yi, X. Peng, H. Zhang, W. Zhang, R. J. G. Hulswit, N. Loman, A. Rambaut, C. Ke, T. A. Bowden, O. G. Pybus, and J. Lu. Identification of common deletions in the spike protein of severe acute respiratory syndrome coronavirus 2. *J Virol*, **94**(17), 2020. ISSN 1098-5514 (Electronic) 0022-538X (Linking). https://doi.org/10.1128/JVI.00790-20. URL https://www.ncbi.nlm.nih.gov/pubmed/32571797.
10. Y. Weisblum, F. Schmidt, F. Zhang, J. DaSilva, D. Poston, J. C. Lorenzi, F. Muecksch, M. Rutkowska, H. H. Hoffmann, E. Michailidis, C. Gaebler, M. Agudelo, A. Cho, Z. Wang, . Gazumyan, M. Cipolla, L. Luchsinger, C. D. Hillyer, M. Caskey, D. F. Robbiani, C. M. Rice, M. C. Nussenzweig, T. Hatziioannou, and P. D. Bieniasz. Escape from neutralizing antibodies by SARS-CoV-2 spike protein variants. *Elife*, **9**, 2020. ISSN 2050-084X (Electronic) 2050-084X (Linking). https://doi.org/10.7554/eLife.61312. URL https://www.ncbi.nlm.nih.gov/pubmed/33112236.
11. E. Andreano, G. Piccini, D. Licastro, L. Casalino, N. V. Johnson, I. Paciello, S. D. Monego, E. Pantano, N. Manganaro, A. Manenti, R. Manna, E. Casa, I. Hyseni, L. Benincasa, E. Montomoli, R. E. Amaro, J. S. McLellan, and R. Rappuoli. SARS-CoV-2 escape in vitro from a highly neutralizing Covid-19 convalescent plasma. *bioRxiv*, 2020. https://doi.org/10.1101/2020.12.28.424451. URL https://www.ncbi.nlm.nih.gov/pubmed/33398278.
12. Zhuoming Liu, Laura A. VanBlargan, Louis-Marie Bloyet, Paul W. Rothlauf, Rita E. Chen, Spencer Stumpf, Haiyan Zhao, John M. Errico, Elitza S. Theel, Mariel J. Liebeskind, Brynn Alford, William J. Buchser, Ali H. Ellebedy, Daved H. Fremont, Michael S. Diamond, and Sean P. J. Whelan. Landscape analysis of escape variants identifies SARS-CoV-2 spike mutations that attenuate monoclonal and serum antibody neutralization. *bioRxiv*, page 2020.11.06.372037, 2021. https://doi.org/10.1101/2020.11.06.372037. URL https://www.biorxiv.org/content/biorxiv/early/2021/01/11/2020.11.06.372037.full.pdf.
13. A. J. Greaney, A. N. Loes, K. H. D. Crawford, T. N. Starr, K. D. Malone, H. Y. Chu, and J. D. Bloom. Comprehensive mapping of mutations in the SARS-CoV-2 receptor-binding domain that affect recognition by polyclonal human plasma antibodies. *Cell Host Microbe*, **29**(3):463–476 e6, 2021. ISSN 1934-6069 (Electronic) 1931-3128 (Linking). https://doi.org/10.1016/j.chom.2021.02.003. URL https://www.ncbi.nlm.nih.gov/pubmed/33592168.
14. X. Xie, Y. Liu, J. Liu, X. Zhang, J. Zou, C. R. Fontes-Garfias, H. Xia, K. A. Swanson, M. Cutler, D. Cooper, V. D. Menachery, S. C.Weaver, P. R. Dormitzer, and P. Y. Shi. Neutralization of SARSCoV-2 spike 69/70 deletion, E484K and N501Y variants by BNT162b2 vaccine-elicited sera. *Nat Med*, 2021. ISSN 1546-170X (Electronic) 1078-8956 (Linking). https://doi.org/10.1038/s41591-021-01270-4. URL https://www.ncbi.nlm.nih.gov/pubmed/33558724.
15. Z. Wang, F. Schmidt, Y. Weisblum, F. Muecksch, C. O. Barnes, S. Finkin, D. Schaefer-Babajew, M. Cipolla, C. Gaebler, J. A. Lieberman, T. Y. Oliveira, Z. Yang, M. E. Abernathy, K. E. Huey-Tubman, A. Hurley, M. Turroja, K. A. West, K. Gordon, K. G. Millard, V. Ramos, J. D. Silva, J. Xu, R. A. Colbert, R. Patel, J. Dizon, C. Unson-O'Brien, I. Shimeliovich, A. Gazumyan, M. Caskey, P. J. Bjorkman, R. Casellas, T. Hatziioannou, P. D. Bieniasz, and M. C. Nussenzweig. mRNA vaccine-elicited antibodies to SARS-CoV-2 and circulating variants. *Nature*, 2021. ISSN 1476-4687 (Electronic) 0028-0836 (Linking). https://doi.org/10.1038/s41586-021-03324-6. URL https://www.ncbi.nlm.nih.gov/pubmed/33567448.
16. K. Wu, A. P. Werner, M. Koch, A. Choi, E. Narayanan, G. B. E. Stewart-Jones, T. Colpitts, H. Bennett, S. Boyoglu-Barnum, W. Shi, J. I. Moliva, N. J. Sullivan, B. S. Graham, A. Carfi, K. S. Corbett, R. A. Seder, and D. K. Edwards. Serum neutralizing activity elicited by mRNA-1273 vaccine - preliminary report. *N Engl J Med*, 2021. ISSN 1533-4406 (Electronic) 0028-4793 (Linking). https://doi.org/10.1056/NEJMc2102179. URL https://www.ncbi.nlm.nih.gov/pubmed/33596346.
17. Y. Liu, J. Liu, H. Xia, X. Zhang, C. R. Fontes-Garfias, K. A. Swanson, H. Cai, R. Sarkar, W. Chen, M. Cutler, D. Cooper, S. C. Weaver, A. Muik, U. Sahin, K. U. Jansen, X. Xie, P. R. Dormitzer, and P. Y. Shi. Neutralizing activity of BNT162b2-elicited serum - preliminary report. *N Engl J Med*, 2021. ISSN 1533-4406 (Electronic) 0028-4793 (Linking). https://doi.org/10.1056/NEJMc2102017. URL https://www.ncbi.nlm.nih.gov/pubmed/33596352.
18. W. F. Garcia-Beltran, E. C. Lam, M. G. Astudillo, D. Yang, T. E. Miller, J. Feldman, B. M. Hauser, T. M. Caradonna, K. L. Clayton, A. D. Nitido, M. R. Murali, G. Alter, R. C. Charles, A. Dighe, J. A. Branda, J. K. Lennerz, D. Lingwood, A. G. Schmidt, A. J. Iafrate, and A. B. Balazs. Covid-19-neutralizing antibodies predict disease severity and survival. *Cell*, **184**(2):476–488 e11, 2021. ISSN 1097-4172 (Electronic) 0092-8674 (Linking). https://doi.org/10.1016/j.cell.2020.12.015. URL https://www.ncbi.nlm.nih.gov/pubmed/33412089.
19. Constantinos Kurt Wibmer, Frances Ayres, Tandile Hermanus, Mashudu Madzivhandila, Prudence Kgagudi, Bronwen E. Lambson, Marion Vermeulen, Karin van den Berg, Theresa Rossouw, Michael Boswell, Veronica Ueckermann, Susan Meiring, Anne von Gottberg, Cheryl Cohen, Lynn Morris, Jinal N. Bhiman, and Penny L. Moore. SARSCoV-2 501Y.V2 escapes neutralization by South African Covid-19 donor plasma. *bioRxiv*, page 2021.01.18.427166, 2021. https://doi.org/10.1101/2021.01.18.427166. URL https://www.biorxiv.org/content/biorxiv/early/2021/01/19/2021.01.18.427166.full.pdf.
20. Markus Hoffmann, Prerna Arora, Rüdiger Groß, Alina Seidel, Bojan Hörnich, Alexander Hahn, Nadine Krüger, Luise Graichen, Heike Hofmann-Winkler, Amy Kempf, Martin Sebastian Winkler, Sebastian Schulz, Hans-Martin Jäck, Bernd Jahrsdörfer, Hubert Schrezenmeier, Martin Müller, Alexander Kleger, Jan Münch, and Stefan Pöhlmann. SARS-CoV-2 variants B.1.351 and B.1.1.248: Escape from therapeutic antibodies and antibodies induced by infection and vaccination. *bioRxiv*, 2021. https://doi.org/10.1101/2021.02.11.430787. URL https://www.biorxiv.org/content/early/2021/02/11/2021.02.11.430787.
21. Delphine Planas, Timothée Bruel, Ludivine Grzelak, Florence Guivel-Benhassine, Isabelle Staropoli, Françoise Porrot, Cyril Planchais, Julian Buchrieser, Maaran Michael Rajah, Elodie Bishop, Mélanie Albert, Flora Donati, Sylvie Behillil, Vincent Enouf, Marianne Maquart, Maria Gonzalez, Jérôme De Sèze, Hélène Péré, David Veyer, Aymeric Sève, Etienne Simon-Lorière, Samira Fafi-Kremer, Karl Stefic, Hugo Mouquet, Laurent Hocqueloux, Sylvie van der Werf, Thierry Prazuck, and Olivier Schwartz. Sensitivity of infectious SARS-CoV-2 B.1.1.7 and B.1.351 variants to neutralizing antibodies. *bioRxiv*, 2021. https://doi.org/10.1101/2021.02.12.430472. URL https://www.biorxiv.org/content/early/2021/02/12/2021.02.12.430472.
22. T. Skelly Donal, C. Harding Adam, Gilbert-Jaramillo Javier, L. Knight Michael, Longet Stephanie, Anthony Brown, Adele Sandra, Adland Emily, Brown Helen, Team Medawar Laboratory, Tom Tipton, Stafford Lizzie, A. Johnson Síle, Amini Ali, Optic Clinical Group, Kit Tan Tiong, Schimanski Lisa, A. Huang Kuan-Ying, Rijal Pramila, Pitch Study Group, Cmore Phosp-C. Group, Frater John, Goulder Philip, P. Conlon Christopher, Jeéry Katie, Dold Christina, J. Pollard Andrew, R. Townsend Alain, Klenerman Paul, J. Dunachie Susanna, Barnes Eleanor, W. Carroll Miles, and S. James William. *Research Square*, 2021. ISSN 2693-5015. https://doi.org/10.21203/rs.3.rs-226857/v1. URL https://doi.org/10.21203/rs.3.rs-226857/v1.
23. P. Wang, L. Liu, S. Iketani, Y. Luo, Y. Guo, M. Wang, J. Yu, B. Zhang, P. D. Kwong, B. S. Graham, J. R. Mascola, J. Y. Chang, M. T. Yin, M. Sobieszczyk, C. A. Kyratsous, L. Shapiro, Z. Sheng, M. S. Nair, Y. Huang, and D. D. Ho. Increased resistance of SARS-CoV-2 variants B.1.351 and B.1.1.7 to antibody neutralization. *bioRxiv*, 2021. https://doi.org/10.1101/2021.01.25.428137. URL https://www.ncbi.nlm.nih.gov/pubmed/33532778.
24. Farina Karim, Inbal Gazy, Sandile Cele, Yenzekile Zungu, Robert Krause, Mallory Bernstein, Yashica Ganga, Hylton Rodel, Ntombifuthi Mthabela, Matilda Mazibuko, Khadija Khan, Daniel Muema, Dirhona Ramjit, Gila Lustig, Thumbi Ndung'u, Willem Hanekom, Bernadett I. Gosnell, Emily Wong, Tulio de Oliveira, Mahomed-Yunus S. Moosa, Alasdair Leslie, Henrik Kløverpris, and Alex Sigal. HIV infection alters SARSCoV-2 responsive immune parameters but not clinical outcomes in Covid-19 disease. *medRxiv*, page 2020.11.23.20236828, 2020. https://doi.org/10.1101/2020.11.23.20236828. URL https://www.medrxiv.org/content/medrxiv/early/2020/11/24/2020.11.23.20236828.full.pdf.
25. C. Gaebler, Z. Wang, J. C. C. Lorenzi, F. Muecksch, S. Finkin, M. Tokuyama, A. Cho, M. Jankovic, D. Schaefer-Babajew, T. Y. Oliveira, M. Cipolla, C. Viant, C. O. Barnes, Y. Bram, G. Breton, T. Hagglof, P. Mendoza, A. Hurley, M. Turroja, K. Gordon, K. G. Millard, V. Ramos, F. Schmidt, Y. Weisblum, D. Jha, M. Tankelevich, G. Martinez-Delgado, J. Yee, R. Patel, J. Dizon, C. Unson- O'Brien, I. Shimeliovich, D. F. Robbiani, Z. Zhao, A. Gazumyan, R. E. Schwartz, T. Hatziioannou, P. J. Bjorkman, S. Mehandru, P. D. Bieniasz, M. Caskey, and M. C. Nussenzweig. Evolution of antibody immunity to SARS-CoV-2, 2021. ISSN 1476-4687 (Electronic) 0028-0836 (Linking). URL https://www.ncbi.nlm.nih.gov/pubmed/33461210.
26. James Brett Case, Adam L Bailey, Arthur S Kim, Rita E Chen, and Michael S Diamond. Growth, detection, quanti_cation, and inactivation of SARS-CoV-2. *Virology*, 2020.
27. A. Sigal, J. T. Kim, A. B. Balazs, E. Dekel, A. Mayo, R. Milo, and D. Baltimore. Cell-to-cell spread of HIV permits ongoing replication despite antiretroviral therapy. *Nature*, **477**(7362):95–8, 2011. ISSN 1476-4687 (Electronic) 0028-0836 (Linking). https://doi.org/10.1038/nature10347. URL https://www.ncbi.nlm.nih.gov/pubmed/21849975.
28. L. Shen, S. Peterson, A. R. Sedaghat, M. A. McMahon, M. Callender, H. Zhang, Y. Zhou, E. Pitt, K. S. Anderson, E. P. Acosta, and R. F. Siliciano. Dose-response curve slope sets class-specific limits on inhibitory potential of anti-HIV drugs. *Nat Med*, **14**(7):762–6, 2008. ISSN 1546-170X (Electronic) 1078-8956 (Linking). https://doi.org/10.1038/nm1777. URL https://www.ncbi.nlm.nih.gov/pubmed/18552857.
29. A. Tarke, J. Sidney, C. K. Kidd, J. M. Dan, S. I. Ramirez, E. D. Yu, J. Mateus, R. da Silva Antunes, E. Moore, P. Rubiro, N. Methot, E. Phillips, S. Mallal, A. Frazier, S. A. Rawlings, J. A. Greenbaum, B. Peters, D. M. Smith, S. Crotty, D. Weiskopf, A. Grifoni, and A. Sette. Comprehensive analysis of t cell immunodominance and immunoprevalence of SARS-CoV-2 epitopes in Covid-19 cases. *Cell Rep Med*, **2**(2):100204, 2021. ISSN 2666-3791 (Electronic) 2666-3791 (Linking). https://doi.org/10.1016/j.xcrm.2021.100204. URL https://www.ncbi.nlm.nih.gov/pubmed/33521695.

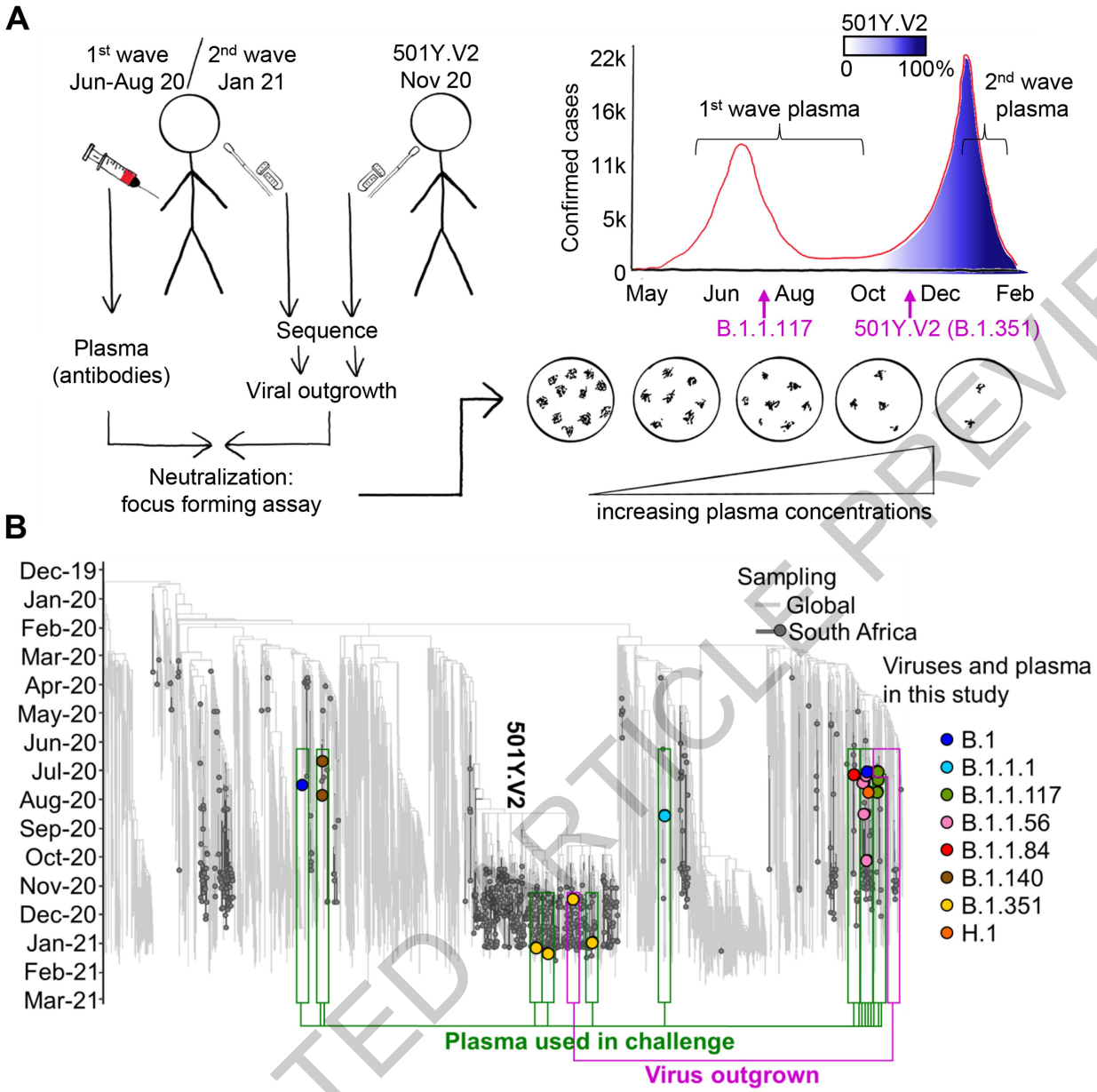

Sequence ID	Accession ID	Variant ID	PANGO lineage	Spike aa substitutions	Spike deletions
K002868	EPI_ISL_602622	SARSCoV2.V003	B.1.1.117	S: D614G S: A688V	-
K005325	EPI_ISL_678615	501Y.V2.HV001	B.1.351	S: L18F S: D80A S: D215G S: K417N S: E484K S: N501Y S: D614G S: A701V	S: 242-244del

Fig. 1 | Study design and sequences of SARS-CoV-2 variants. (A) We obtained convalescent plasma and sequenced the matching infecting virus in the first and second SARS-CoV-2 infection waves in South Africa. A first wave variant lacking the 501Y.V2 RBD and NTD mutations was outgrown from one participant infected in the first South African infection wave, and 501Y.V2 was outgrown from a participant at the beginning of the second wave. Neutralization was by: i) first wave plasma of first wave virus; ii) second wave plasma of 501Y.V2 virus; iii) first wave plasma of 501Y.V2 virus; iv) second wave plasma of first wave virus. A focus forming live virus neutralization assay (LVNA) was used to quantify neutralization. (B) Phylogenetic relationships and mutations in virus sequences. Variants which elicited the antibody immunity in the plasma samples are highlighted in green boxes. Variants which were outgrown are highlighted in magenta boxes. Y-axis denotes time of sampling. Table shows mutations present in spike for the SARS-CoV-2 outgrown variants used in the LVNA. See Extended Data Table 2 for a complete list of mutations in the viral genomes of variants eliciting plasma immunity and outgrown variants.

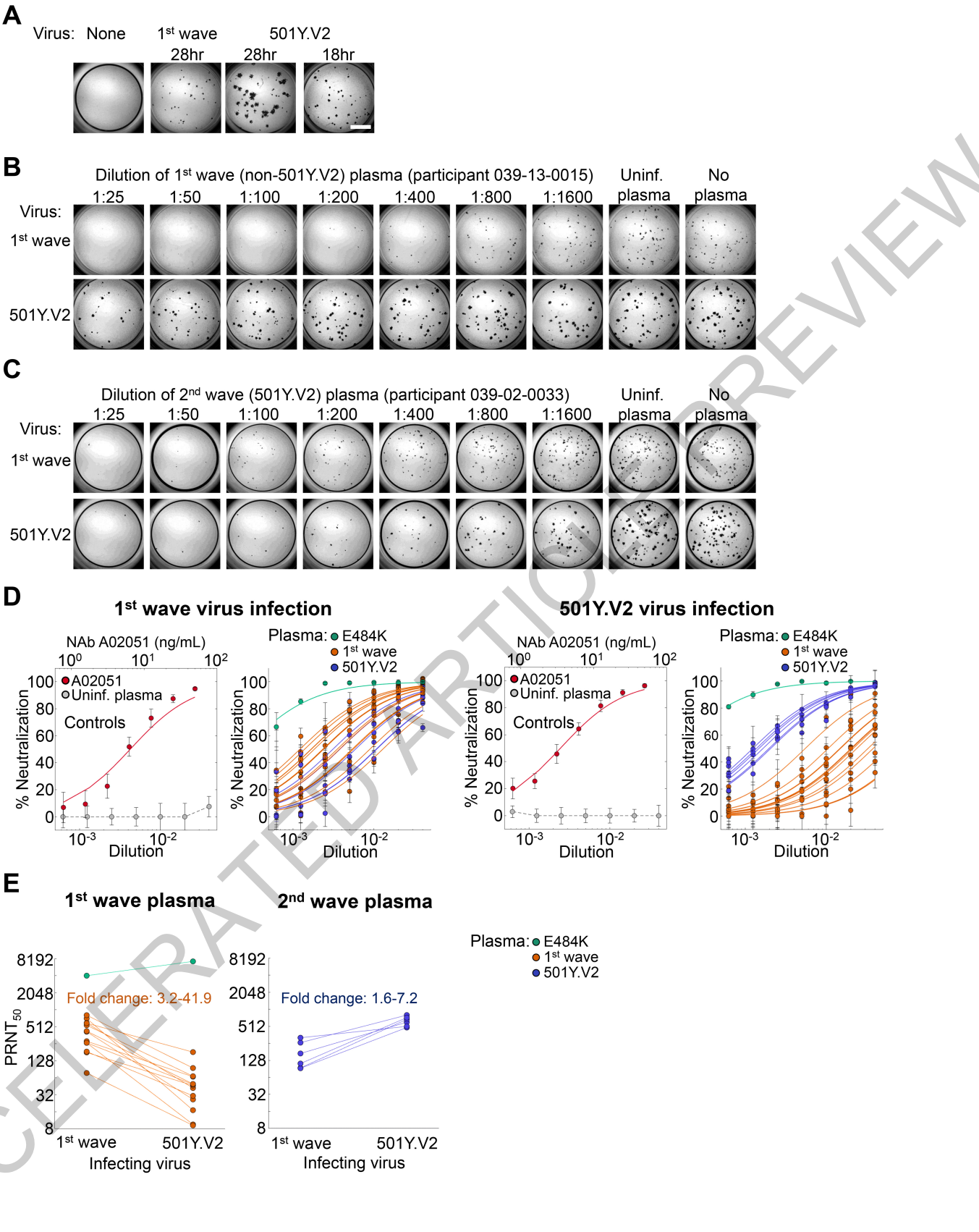

Fig. 2 | Neutralization of first South African infection wave and 501Y.V2 variants by convalescent plasma elicited by first wave and 501Y.V2 infections. (A) Focus formation by first wave versus 501Y.V2 virus. To obtain similar focus size, 501Y.V2 incubation time was reduced to 18 hours. Scale bar 2mm. A representative focus forming assay using plasma from first wave infected participant 039-13-0015 (B) or 501Y.V2 infected participant 039-02-0033 (C). Columns are plasma dilutions, ranging from 1:25 to 1:1600, a plasma pool from 3 uninfected individuals, and a no plasma control. (D) Quantified neutralization per participant. Bright red points are neutralization by A02051 NAb, grey points neutralization by uninfected plasma, green points neutralization by E484K mutant virus elicited plasma, red points neutralization by plasma from participants infected by first wave, non-501Y.V2 variants, and blue points are neutralization by plasma from 501Y.V2 infected participants. Mean and s.e. of 3-4 independent experiments per participant convalescent plasma from the first (n = 14) or second (n = 6) infection wave or 10 independent experiments for controls. Solid lines of the corresponding colour are fitted values using a sigmoidal equation. First plot shows neutralization of first wave virus by A02051 ($PRNT_{50}$ = 6.5 ng/mL, 95% confidence intervals of 3.9–9.1 ng/mL) and uninfected plasma. Second plot is neutralization of first wave virus by plasma from convalescent participants. Third plot is neutralization of the 501Y.V2 by A02051 ($PRNT_{50}$ = 3.5 ng/mL (2.9–4.1 ng/mL)) and uninfected plasma. Forth plot is neutralization of 501Y.V2 virus by plasma from convalescent participants. (E) Decline in $PRNT_{50}$ in cross-neutralization. Left plot is first wave plasma neutralization of first wave versus 501Y.V2 virus, right plot is second wave plasma neutralization of 501Y.V2 versus first wave virus. Fold-change decline ranged from 3.2–41.9 for first wave plasma, and 1.6–7.2 for second wave plasma. Fold-change elicited by E484K was excluded.

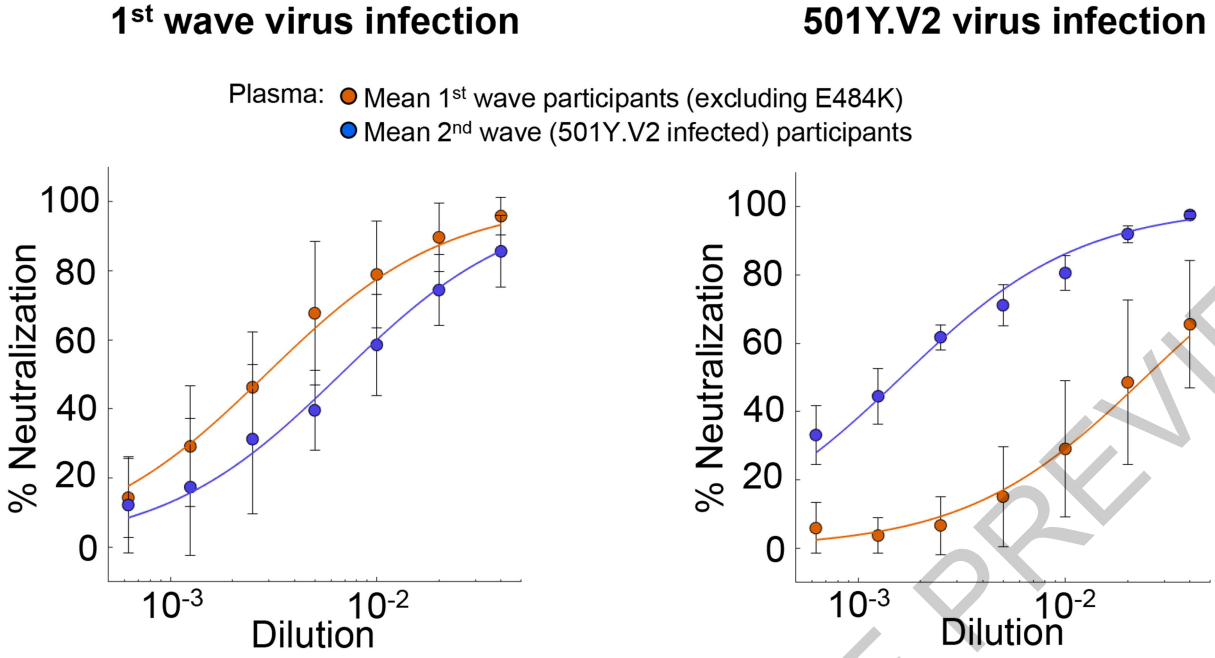

Plasma $PRNT_{50}$

Virus variant	Plasma source: 1st wave	Plasma source: 501Y.V2	Fold change HM/HT
1st wave	344.0 (275.4-458.0)	149.7 (132.1-172.8)	2.3
501Y.V2	41.1 (32.7-55.5)	619.7 (517.8-771.5)	15.1
Fold change HM/HT	8.4	4.1	

Homologous (HM)
Heterologous (HT)

Fig. 3 | Cross-neutralization of first infection wave and 501Y.V2 virus across all participants. Left plot shows neutralization of first wave virus, right plot shows neutralization of 501Y.V2. Sigmoidal fits were performed to the means of first (red points) and second wave (blue points) plasma neutralization results across all participants excluding participant with plasma immunity elicited by virus with the E484K mutation alone. Shown are means and standard deviations of n = 13 first wave infected plasma donors and n = 6 second wave infected plasma donors. Summary table shows plasma $PRNT_{50}$ as a function of plasma source (columns) and infecting viral variant (rows). Blue rectangles highlight homologous neutralization where virus and infection wave are matched, and yellow rectangles highlight cross-neutralization where virus and plasma are from different infection waves.

Methods

Ethical statement

Nasopharyngeal/oropharyngeal swab samples and plasma samples were obtained from 20 hospitalized adults with PCR-confirmed SARS-CoV-2 infection enrolled in a prospective cohort study approved by the Biomedical Research Ethics Committee (BREC) at the University of KwaZulu-Natal (reference BREC/00001275/2020). The 501Y.V2 variant was obtained from a residual nasopharyngeal/oropharyngeal sample used for routine SARS-CoV-2 diagnostic testing by the National Health Laboratory Service, through our SARS-CoV-2 genomic surveillance program (BREC approval reference BREC/00001510/2020).

Data and code availability statement

Sequence data that support the findings of this study have been deposited in GISAID with accession codes as listed in Extended Data Table 2 The sequence analysis and visualization pipeline is available on GitHub (https://github.com/nextstrain/ncov). Image analysis and curve fitting scripts in Matlab 2019b are available on GitHub (https://github.com/sigallab/NatureMarch2021). Raw images are available from the corresponding author upon reasonable request.

Whole genome sequencing, genome assembly and phylogenetic analysis

cDNA synthesis was performed on the extracted RNA using random primers followed by gene specific multiplex PCR using the ARTIC V3 protocol. Briefly, extracted RNA was converted to cDNA using the Superscript IV First Strand synthesis system (Life Technologies, Carlsbad, CA) and random hexamer primers. SARS-CoV-2 whole genome amplification was performed by multiplex PCR using primers designed on Primal Scheme (http://primal.zibraproject.org/) to generate 400bp amplicons with an overlap of 70bp that covers the 30Kb SARS-CoV-2 genome. PCR products were cleaned up using AmpureXP purification beads (Beckman Coulter, High Wycombe, UK) and quantified using the Qubit dsDNA High Sensitivity assay on the Qubit 4.0 instrument (Life Technologies Carlsbad, CA). We then used the Illumina® Nextera Flex DNA Library Prep kit according to the manufacturer's protocol to prepare indexed paired end libraries of genomic DNA. Sequencing libraries were normalized to 4nM, pooled and denatured with 0.2N sodium acetate. 12pM sample library was spiked with 1% PhiX (PhiX Control v3 adapter-ligated library used as a control). We sequenced libraries on a 500-cycle v2 MiSeq Reagent Kit on the Illumina MiSeq instrument (Illumina, San Diego, CA). We assembled paired-end fastq reads using Genome Detective 1.126 (https://www.genomedetective.com) and the Coronavirus Typing Tool. We polished the initial assembly obtained from Genome Detective by aligning mapped reads to the references and filtering out low-quality mutations using the bcftools 1.7–2 mpileup method. Mutations were confirmed visually with bam files using Geneious software (Biomatters Ltd, Auckland, New Zealand). All of the sequences were deposited in GISAID (https://www.gisaid.org/). We retrieved all South African SARS-CoV-2 genotypes from the GISAID database as of 11 January 2021 (N = 2704). We initially analyzed South African genotypes against the global reference dataset (N = 2592) using a custom pipeline based on a local version of NextStrain. The pipeline contains several python scripts that manage the analysis workflow. It performs alignment of genotypes in MAFFT, phylogenetic tree inference in IQ-Tree20, tree dating and ancestral state construction and annotation (https://github.com/nextstrain/ncov).

Cells

Vero E6 cells (ATCC CRL-1586, obtained from Cellonex in South Africa) were propagated in complete DMEM with 10% fetal bovine serum (Hylone) containing 1% each of HEPES, sodium pyruvate, L-glutamine, and non-essential amino acids (Sigma-Aldrich). Cells were passaged every 3–4 days. H1299 cells were propagated in complete RPMI with 10% fetal bovine serum containing 1% each of HEPES, sodium pyruvate, L-glutamine, and non-essential amino acids and and passaged every second day. HEK-293 (ATCC CRL-1573) cells were propagated in complete DMEM with 10% fetal bovine serum containing 1% each of HEPES, sodium pyruvate, L-glutamine, and non-essential amino acids and and passaged every second day.Cell lines have not been authenticated. The cell lines have been tested for mycoplasma contamination and are mycoplasma negative.

H1299-E3 cell line for first passage SARS-CoV-2 outgrowth

The H1299-H2AZ clone with nuclear labelled YFP was constructed to overexpress ACE2 as follows: VSVG-pseudotyped lentivirus containing the human ACE2 was generated by co-transfecting 293T cells with the pHAGE2-EF1alnt-ACE2-WT plasmid along with the lentiviral helper plasmids HDM-VSVG, HDM-Hgpm2, HDM-tat1b and pRC-CMV-Rev1b using TransIT-LT1 (Mirus) transfection reagent. Supernatant containing the lentivirus was harvested two days after infection, filtered through a 0.45 μm filter (Corning) and used to spinfect H1299-H2AZ at 1000 rcf for 2 hours at room temperature in the presence of 5 μg/mL polybrene (Sigma-Aldrich). ACE-2 transduced H1299-H2AZ cells were then subcloned at the single cell density in 96-well plates (Eppendorf) in conditioned media derived from confluent cells. After 3 weeks, wells were trypsinized (Sigma-Aldrich) and plated in two replicate plates, where the first plate was used to determine infectivity and the second was stock. The first plate was screened for the fraction of mCherry positive cells per cell clone upon infection with SARS-CoV-2 mCherry expressing spike pseudotyped lentiviral vector 1610-pHAGE2/EF1a Int-mCherry3-W produced by transfecting as above. Screening was performed using a Metamorph-controlled (Molecular Devices, Sunnyvale, CA) Nikon TiE motorized microscope (Nikon Corporation, Tokyo, Japan) with a 20x, 0.75 NA phase objective, 561 laser line, and 607 nm emission filter (Semrock, Rochester, NY). Images were captured using an 888 EMCCD camera (Andor). Temperature (37 °C), humidity and CO2 (5%) were controlled using an environmental chamber (OKO Labs, Naples, Italy). The clone with the highest fraction of mCherry expression was expanded from the stock plate and denoted H1299-E3. This clone was used in the outgrowth.

Viral Outgrowth

All live virus work was performed in Biosafety level 3 containment using Africa Health Research Institute biosafety committee approved protocols for SARS-CoV-2. For first wave virus, a T25 flask (Corning) was seeded with Vero E6 cells at 2×10^5 cells/ml and incubated for 18–20 hours. After 1 DPBS wash, the sub-confluent cell monolayer was inoculated with 500 μL universal transport medium (UTM) diluted 1:1 with growth medium and filtered through a 0.45 μM filter. Cells were incubated for 1 hour. Flask was then filled with 7 mL of complete growth medium and checked daily for cytopathic effect (CPE). Four days post infection, supernatants of the infected culture were collected, centrifuged at 300 rcf for 3 minutes to remove cell debris, and filtered using a 0.45 μM filter. Viral supernatant was aliquoted and stored at −80 °C. For 501Y.V2 variants, we used H1299-ACE2-E3 cells for initial isolation followed by passage into Vero E6 cells. H1299-ACE2-E3 cells were seeded at 1.5×10^5 cells/ml and incubated for 18–20 hours. After 1 DPBS wash, the sub-confluent cell monolayer was inoculated with 500 μL universal transport medium (UTM) diluted 1:1 with growth medium and filtered through a 0.45 μM filter. Cells were incubated for 1 hour. Wells were then filled with 3 mL of complete growth medium. 8 days post-infection, cells were trypsinized, centrifuged at 300 rcf for 3 minutes and resuspended in 4 mL growth medium. 1mL was added to Vero E6 cells that had been seeded at t 2×10^5 cells/ml 18–20 hours earlier in a T25 flask (approximately 1:8 donor-to-target cell dilution ratio) for cell-to-cell infection. Coculture of H1299-ACE2-E3 and Vero E6 cells was incubated for 1 hour and flask was then filled with 7 mL of complete growth medium and incubated for 6 days. Viral supernatant

was aliquoted and stored at −80 °C or further passaged in Vero E6 cells as above. Two isolates were outgrown, 501Y.V2.HV001 and 501Y.V2.HVdF002. The second isolate showed fixation of furin cleavage site mutations during outgrowth in Vero E6 cells and was not used except for data presented in Extended Data Figure 1.

Microneutralization using focus forming assay

For plasma from first wave donors, we first quantified spike RBD IgG by enzyme-linked immunosorbent assay (ELISA) using monoclonal antibody CR3022 (used at 4-fold serial dilutions from 1000 ng/mL to 0.244 ng/mL) as a quantitative standard, (n = 13 excluding participant 039-13-0103 for which ELISA data was not available). The mean concentration was 23.7 μg/mL *pm* 19.1 μg/mL, (range 5.7–62.6 μg/mL). In comparison, uninfected donor controls had a mean of 1.85 μg/mL *pm* 0.645 μg/mL. To quantify neutralization, Vero E6 cells were plated in an 96-well plate (Eppendorf or Corning) at 30,000 cells per well 1 day pre-infection. Importantly, before infection approximately 5ml of sterile water was added between wells to prevent more rapid drying of wells at the edge which we have observed to cause edge effects (lower number of foci). Plasma was separated from EDTA-anticoagulated blood by centrifugation at 500 rcf for 10 minutes and stored at −80 °C. Aliquots of plasma samples were heat-inactivated at 56 °C for 30 minutes, and clarified by centrifugation at 10,000 rcf for 5 minutes, where the clear middle layer was used for experiments. Inactivated plasma was stored in single use aliquots to prevent freeze-thaw cycles. For experiments, plasma was serially diluted two-fold from 1:100 to 1:1600, where this is the concentration during the virus-plasma incubation step before addition to cells and during the adsorption step. As a positive control, the GenScript A02051 anti-spike mAb was added at concentrations listed in the figures. Virus stocks were used at approximately 50 focus-forming units (FFU) per microwell and added to diluted plasma; antibody-virus mixtures were incubated for 1 hour at 37 °C, 5% CO2. Cells were infected with 100 μL of the virus-antibody mixtures for one hour, to allow adsorption of virus. Subsequently, 100 μL of a 1x RPMI 1640 (Sigma-Aldrich R6504), 1.5% carboxymethylcellulose (Sigma-Aldrich C4888) overlay was added to the wells without removing the inoculum. Cells were fixed at 28 hours post-infection using 4% paraformaldehyde (Sigma-Aldrich) for 20 minutes. For staining of foci, a rabbit anti-spike monoclonal antibody (mAb BS-R2B12, GenScript A02058) was used at 0.5 μg/mL as the primary detection antibody. Antibody was resuspended in a permiabilization buffer containing 0.1% saponin (Sigma-Aldrich), 0.1% BSA (Sigma-Aldrich), and 0.05% tween (Sigma-Aldrich) in PBS. Plates were incubated with primary antibody overnight at 4 °C, then washed with wash buffer containing 0.05% tween in PBS. Secondary goat anti-rabbit horseradish peroxidase (Abcam ab205718) was added at 1 μg/mL and incubated for 2 hours at room temperature with shaking. The TrueBlue peroxidase substrate (SeraCare 5510-0030) was then added at 50 μL per well and incubated for 20 minutes at room temperature. Plates were then dried for 2 hours and imaged using a Metamorph-controlled Nikon TiE motorized microscope with a 2x objective. Automated image analysis was performed using a Matlab2019b (Mathworks) custom script, where focus detection was automated and did not involve user curation. Image segmentation steps were stretching the image from minimum to maximum intensity, local Laplacian filtering, image complementation, thresholding and binarization. Two plasma donors initially measured from the South African second infection wave did not have detectable neutralization of either 501Y.V2 or the first wave variant and were not used in the study.

Statistics and fitting

All statistics and fitting were performed using Matlab2019b. Neutralization data was fit to $Tx = 1/1 + (D/ID_{50})$.

Here Tx is the number of foci normalized to the number of foci in the absence of plasma on the same plate at dilution D. To visualize the data, we used percent neutralization, calculated as $(1 - Tx) \times 100\%$. Negative values (Tx > 1, enhancement) was represented as 0% neutralization. Fit to a normal distribution used Matlab2019b function normplot, which compared the distribution of the Tx data to the normal distribution (see https://www.mathworks.com/help/stats/normplot.html).

Reporting summary

Further information on research design is available in the Nature Research Reporting Summary linked to this paper.

Acknowledgements This work was supported by the Bill and Melinda Gates Investment INV-018944 (AS) and by the South African Medical Research Council and the Department of Science and Innovation (TdO).

Author contributions Conceived study: AS, TdO, RL, with input from ABB. Designed study and experiments: AS, TdO, SC, SHH, LJ. Performed experiments: SC, IG, JG, YN, SP, and AS. Analyzed and Interpreted data: AS, TdO, SC, HT, EW, GL, MYM, BG, RL. Cohort set-up and management: FK, KK, YG, MB, BG, MYM, SC. AS, TdO, RL, WH, ABB, and SC prepared the manuscript with input from all authors.

Competing interests The authors declare no competing interests.

Additional information

Supplementary information The online version contains supplementary material available at https://doi.org/10.1038/s41586-021-03471-w.

Correspondence and requests for materials should be addressed to T.d.O. or A.S.

Peer review information *Nature* thanks Andreas Radbruch and the other, anonymous, reviewer(s) for their contribution to the peer review of this work. Peer reviewer reports are available.

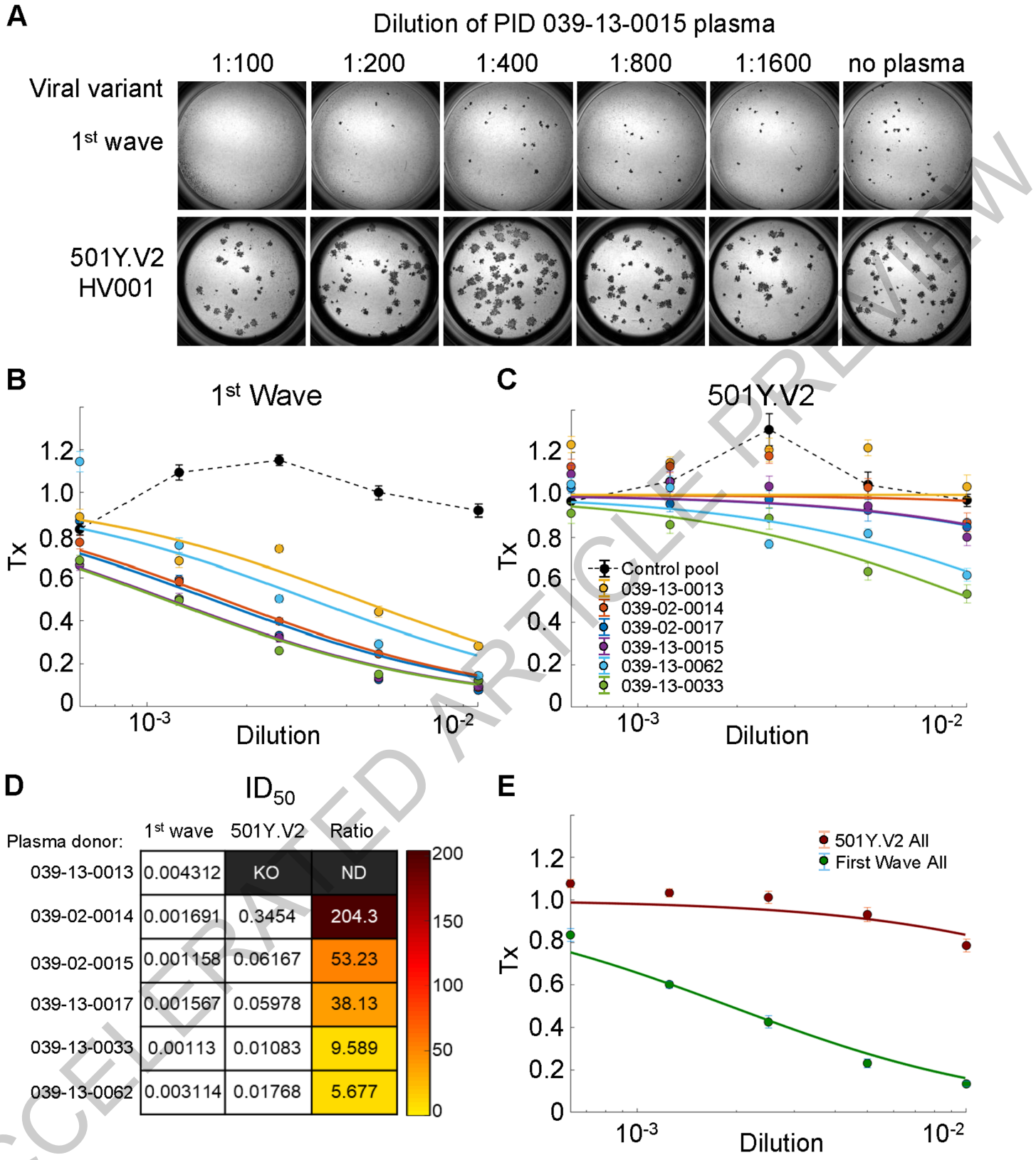

Extended Data Fig. 1 | See next page for caption.

Extended Data Fig. 1 | Neutralization of first wave and 501Y.V2 variants by convalescent plasma from first wave infections using equal infection incubation times. (A) A representative focus forming assay using plasma from participant 039-13-0015. Plasma neutralization of (B) first wave virus and (C) 501Y.V2 variants (501Y.V2.HV001 and 501Y.V2.HVdF002). Colored circles represent means and standard errors from 8 independent neutralization experiments using plasma from n = 6 convalescent participants who were infected by first wave variants in the first peak of the pandemic in South Africa. Correspondingly colored lines are fits of the sigmoidal equation with ID_{50} as the fitted parameter. Data from both 501Y.V2 variants was combined as separate experiments to obtain a more accurate fit of the data using a sigmoidal function since the declines in 501Y.V2 infection were small in the range of plasma concentrations used. The matched infections with first wave virus which were done in parallel with each 501Y.V2 variant were also combined. One experiment was removed in the process of quality control due to plate edge effects, which were subsequently corrected by adding sterile water between wells. Black points represent a pool of plasma from three uninfected controls. The transmission index (Tx) is the number of foci in the presence of the plasma dilution normalized by the number of foci in the absence of plasma. (D) Plasma ID_{50} values and ratios for first wave and 501Y.V2 variants. Knockout (KO) was scored as $ID_{50} > 1$. ND, not defined. (E) Mean and standard error across all plasma donors (n = 6) from 8 independent neutralization experiments.

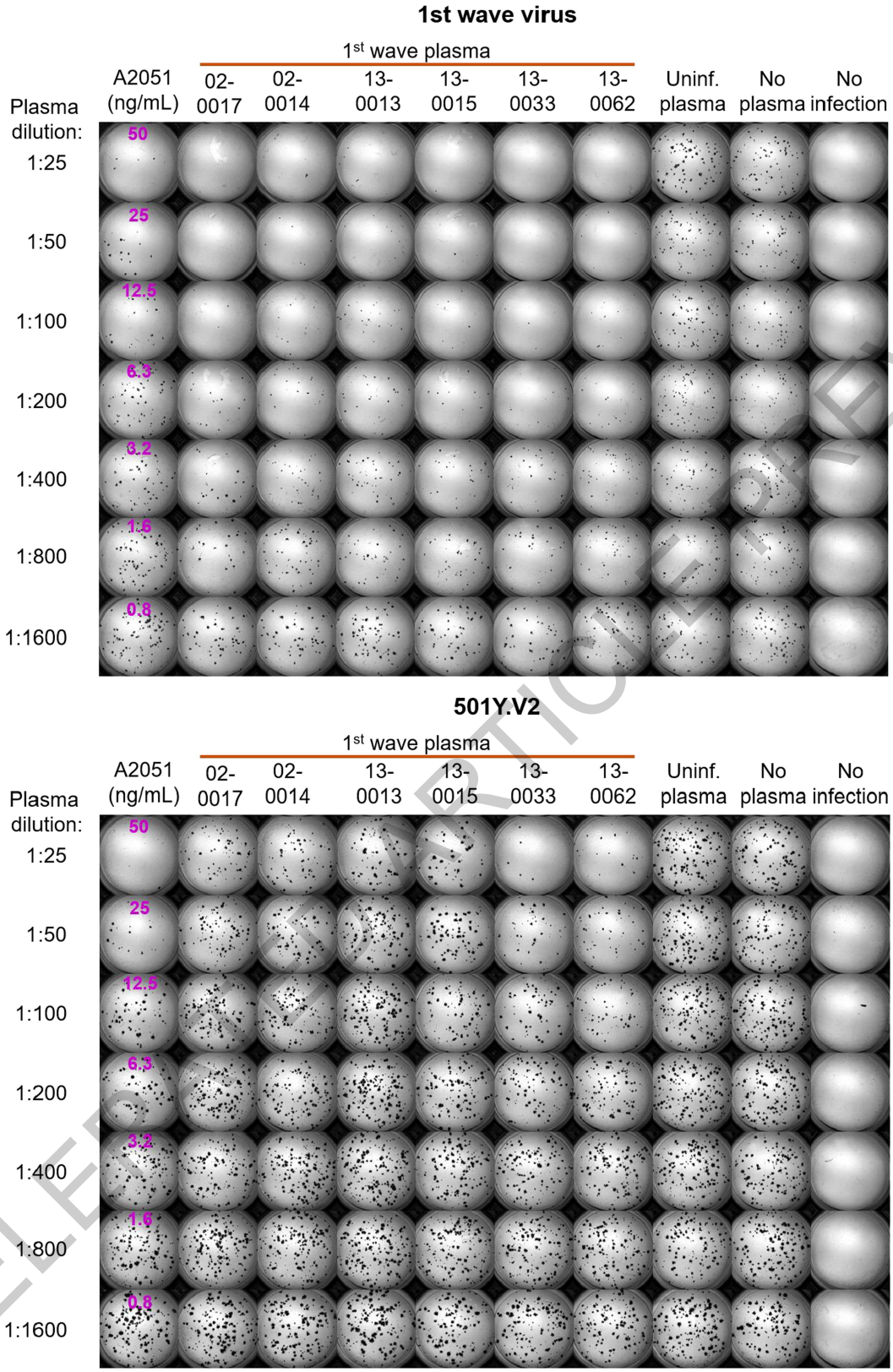

Extended Data Fig. 2 | Neutralization of first wave and 501Y.V2 by convalescent plasma: Representative experiments of first set of participant plasma tested. Top montage shows neutralization of first wave virus, bottom montage shows neutralization of 501Y.V2. Rows are plasma dilutions, ranging from 1:25 to 1:1600. Last three columns are plasma from a pool of uninfected participants, the no plasma control, and no virus, respectively. First column is the A2051 NAb, with antibody concentrations in ng/mL (magenta). First wave plasma donors are marked with a red line, second wave plasma donors are marked with a blue line.

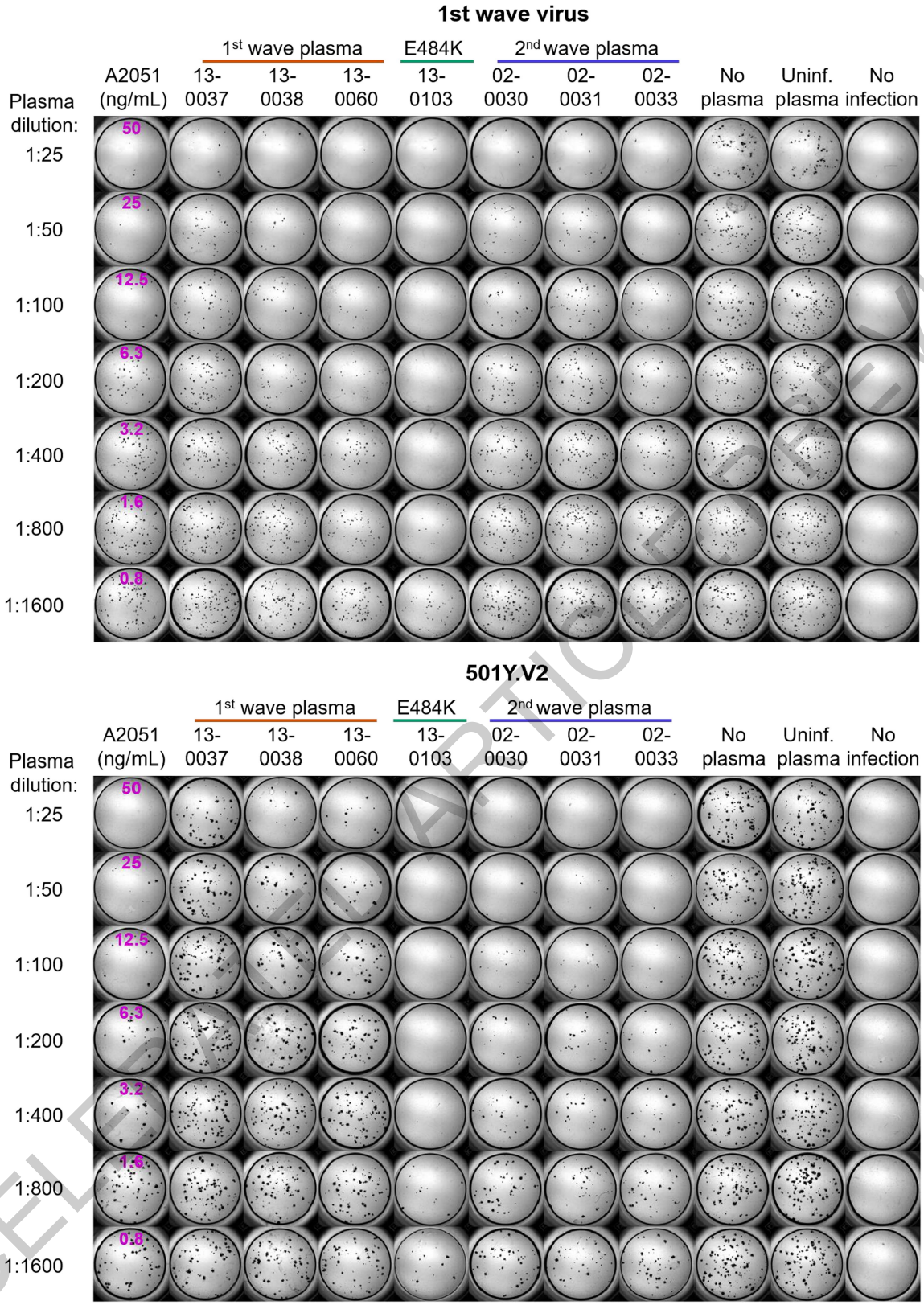

Extended Data Fig. 3 | Neutralization of first wave and 501Y.V2 by convalescent plasma: Representative experiments of second set of participant plasma tested. Top montage shows neutralization of first wave virus, bottom montage shows neutralization of 501Y.V2. Rows are plasma dilutions, ranging from 1:25 to 1:1600. Last three columns are plasma from a pool of uninfected participants, the no plasma control, and no virus, respectively. First column is the A2051 NAb, with antibody concentrations in ng/mL (magenta). First wave plasma donors are marked with a red line, second wave plasma donors are marked with a blue line, the plasma donor showing the E484K mutation only is marked with a green line.

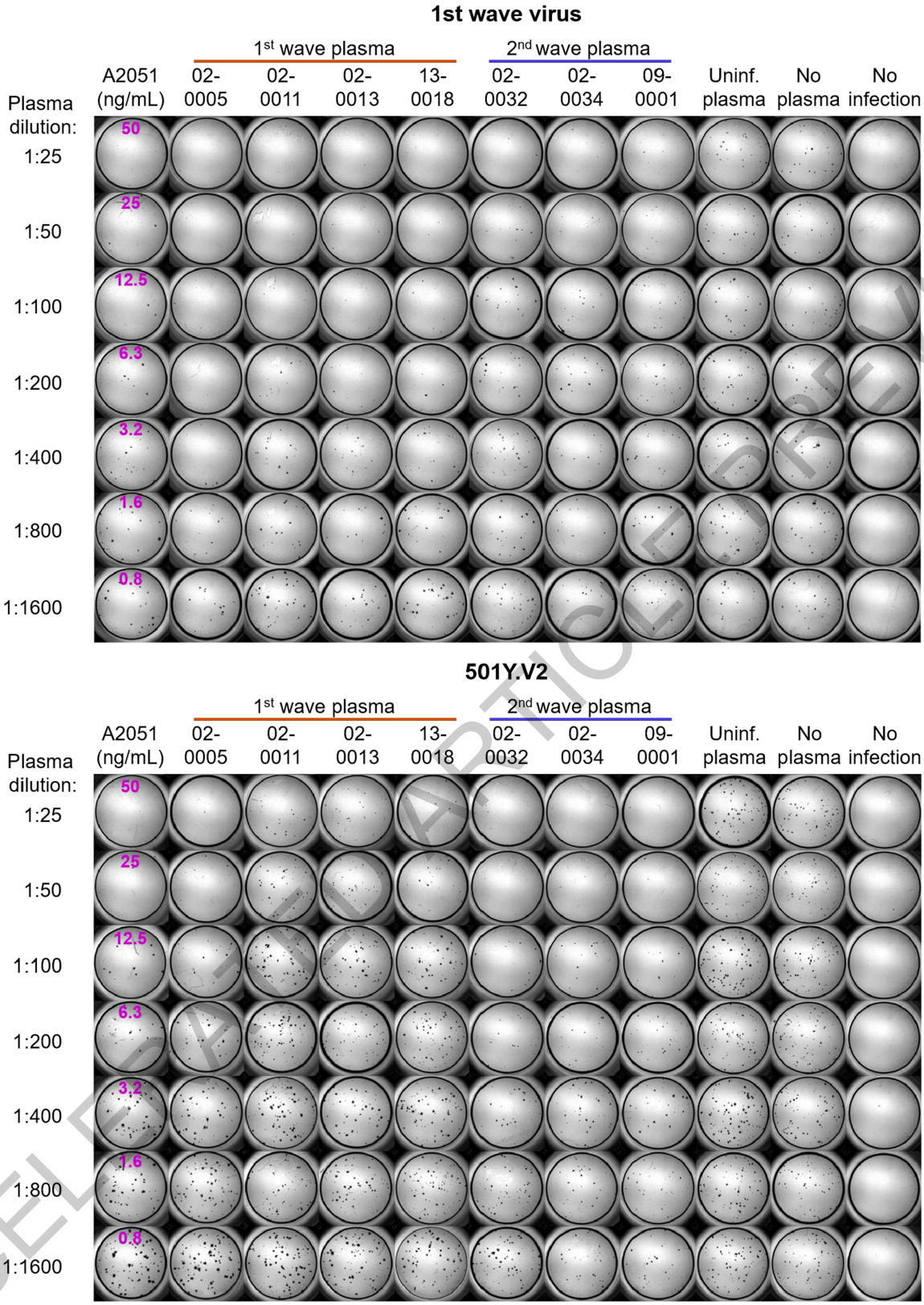

Extended Data Fig. 4 | Neutralization of first wave and 501Y.V2 by convalescent plasma: Representative experiments of third set of participant plasma tested. Top montage shows neutralization of first wave virus, bottom montage shows neutralization of 501Y.V2. Rows are plasma dilutions, ranging from 1:25 to 1:1600. Last three columns are plasma from a pool of uninfected participants, the no plasma control, and no virus, respectively. First column is the A2051 NAb, with antibody concentrations in ng/mL (magenta). First wave plasma donors are marked with a red line, second wave plasma donors are marked with a blue line.

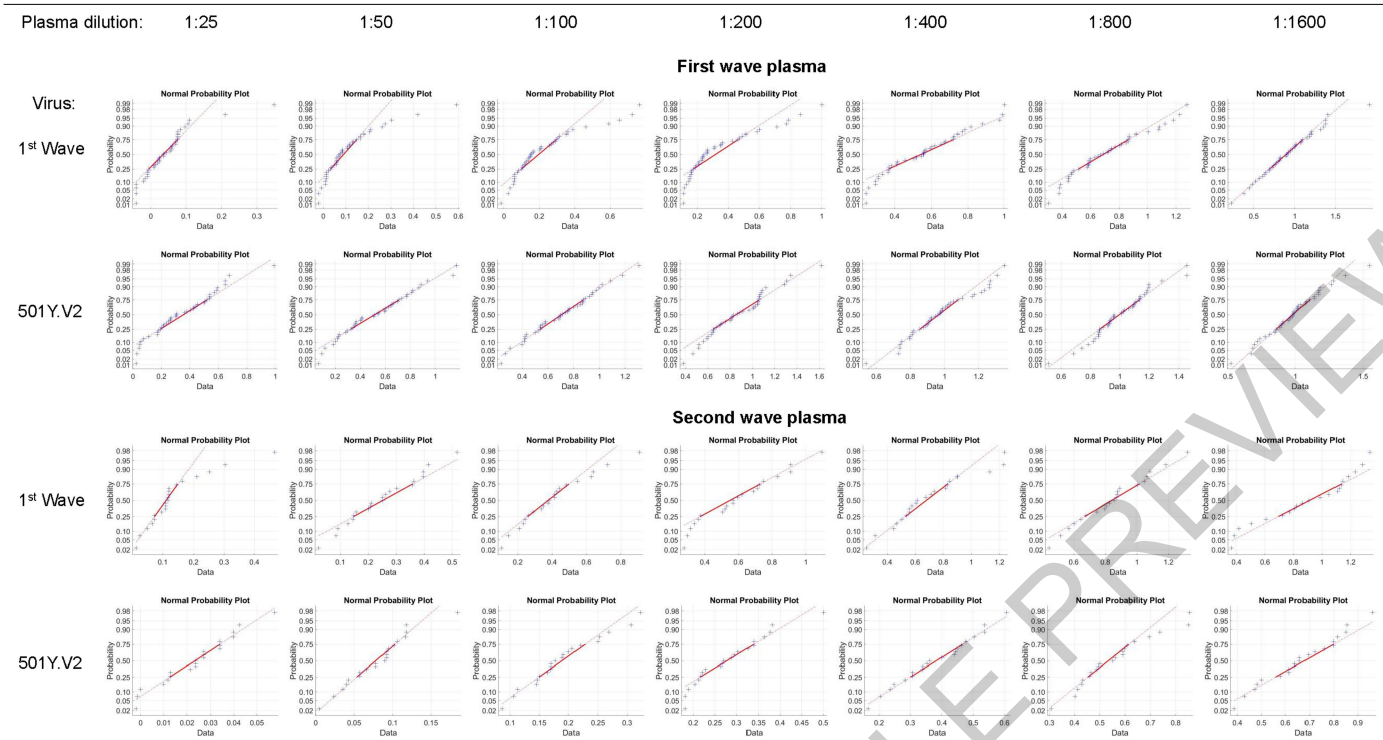

Extended Data Fig. 5 | Fit of combined data for each plasma dilution to a normal distribution. The Matlab2019b function normplot was used to assess the fit of the data (blue crosses) to a normal distribution (solid red line). For each plot, one data point is the Tx result for one experiment for one participant at the specified dilution. Number of total experiments per viral variant was n = 42 for first wave plasma, and n = 21 for second wave plasma. Lack of pronounced curvature of the data in the range of the solid line indicates that a the data is a reasonably good fit to a normal distribution. see https://www.mathworks.com/help/stats/normplot.html for additional information.

Extended Data Table 1 | Plasma donor characteristics

Cohort ID	Sex	Age (yrs)	HIV status	HIV viral load (copies/mL)	Supplemental oxygen	Date of symptom onset	Days between symptom onset and plasma collection	Days between symptom onset and last positive qPCR
039-02-0005	M	50-59	Negative	-	No	14-Jun-20	29	8
039-13-0015	F	40-49	Negative	-	No	21-Jun-20	26	12
039-13-0033	F	30-39	Negative	-	No	24-Jun-20	30	23
039-02-0013	F	70+	Negative	-	Yes	25-Jun-20	29	15
039-13-0013	F	50-59	Positive	<40	No	29-Jun-20	30	10
039-13-0018	F	40-49	Negative	-	No	29-Jun-20	28	14
039-02-0014	F	60-69	Negative	-	No	01-Jul-20	27	20
039-02-0011	F	40-49	Positive	<40	No	03-Jul-20	32	32
039-13-0060	M	40-49	Positive	<40	No	17-Jul-20	38	31
039-02-0017	F	60-69	Negative	-	Yes	21-Jul-20	28	7
039-13-0062	M	60-69	Negative	-	No	06-Aug-20	26	12
039-13-0103	M	60-69	Negative	-	Yes	26-Sep-20	37	17
039-13-0037	M	30-39	Positive	<40	No	Asymptomatic	29*	8†
039-13-0038	M	30-39	Negative	-	No	Asymptomatic	29*	8†
039-02-0031	F	40-49	Negative	-	Yes	26-Dec-20	34	13
039-02-0032	M	40-49	Positive	<40	Yes	27-Dec-20	43	12
039-02-0033	M	50-59	Negative	-	No	28-Dec-20	35	42
039-02-0030	F	40-49	Positive	<40	Yes	29-Dec-20	30	9
039-02-0034	F	30-39	Negative	-	Yes	31-Dec-20	32	5‡
039-09-0001	F	60-69	Negative	-	Yes	11-Jan-21	29	29

*Asymptomatic cases; plasma collected 29 days after positive diagnostic swab for these two participants. †Last positive qPCR collected 8 days after diagnostic swab collection for two participants. ‡Only single qPCR test positive at diagnosis.

nature research

Corresponding author(s): Tulio de Oliveira and Alex Sigal

Last updated by author(s): Mar 15, 2021

Reporting Summary

Nature Research wishes to improve the reproducibility of the work that we publish. This form provides structure for consistency and transparency in reporting. For further information on Nature Research policies, see Authors & Referees and the Editorial Policy Checklist.

Statistics

For all statistical analyses, confirm that the following items are present in the figure legend, table legend, main text, or Methods section.

n/a	Confirmed
☐	☒ The exact sample size (*n*) for each experimental group/condition, given as a discrete number and unit of measurement
☐	☒ A statement on whether measurements were taken from distinct samples or whether the same sample was measured repeatedly
☒	☐ The statistical test(s) used AND whether they are one- or two-sided *Only common tests should be described solely by name; describe more complex techniques in the Methods section.*
☐	☒ A description of all covariates tested
☐	☒ A description of any assumptions or corrections, such as tests of normality and adjustment for multiple comparisons
☐	☒ A full description of the statistical parameters including central tendency (e.g. means) or other basic estimates (e.g. regression coefficient) AND variation (e.g. standard deviation) or associated estimates of uncertainty (e.g. confidence intervals)
☒	☐ For null hypothesis testing, the test statistic (e.g. *F*, *t*, *r*) with confidence intervals, effect sizes, degrees of freedom and *P* value noted *Give P values as exact values whenever suitable.*
☒	☐ For Bayesian analysis, information on the choice of priors and Markov chain Monte Carlo settings
☒	☐ For hierarchical and complex designs, identification of the appropriate level for tests and full reporting of outcomes
☒	☐ Estimates of effect sizes (e.g. Cohen's *d*, Pearson's *r*), indicating how they were calculated

Our web collection on statistics for biologists contains articles on many of the points above.

Software and code

Policy information about availability of computer code

Data collection	Metamorph 7.7.11.0 software for image acquisition of foci. Libraries were sequenced using a 500-cycle v2 MiSeq Reagent Kit on the Illumina MiSeq instrument. Paired-end fastq reads assembled using Genome Detective 1.126.
Data analysis	Matlab 2019b custom scripts for image analysis, fitting, statistics, and graphing. Python and R custom pipeline for sequence analysis, phylogenetic tree generation and visualization. Matlab custom scripts available at https://github.com/sigallab/NatureMarch2021. Pyton and R pipeline available at https://github.com/nextstrain/ncov.

For manuscripts utilizing custom algorithms or software that are central to the research but not yet described in published literature, software must be made available to editors/reviewers. We strongly encourage code deposition in a community repository (e.g. GitHub). See the Nature Research guidelines for submitting code & software for further information.

Data

Policy information about availability of data

All manuscripts must include a data availability statement. This statement should provide the following information, where applicable:

- Accession codes, unique identifiers, or web links for publicly available datasets
- A list of figures that have associated raw data
- A description of any restrictions on data availability

GISAID accession numbers for deposited sequences are: EPI_ISL_602622; EPI_ISL_678615; EPI_ISL_602623; EPI_ISL_660167; EPI_ISL_602629; EPI_ISL_602631; EPI_ISL_602624; EPI_ISL_660170; EPI_ISL_660174; EPI_ISL_660172; EPI_ISL_660173; EPI_ISL_660176; EPISL_660180; EPI_ISL_660181; EPI_ISL_660185; EPI_ISL_1229368; EPI_ISL_1229367.

Field-specific reporting

Please select the one below that is the best fit for your research. If you are not sure, read the appropriate sections before making your selection.

☒ Life sciences ☐ Behavioural & social sciences ☐ Ecological, evolutionary & environmental sciences

For a reference copy of the document with all sections, see nature.com/documents/nr-reporting-summary-flat.pdf

Life sciences study design

All studies must disclose on these points even when the disclosure is negative.

Sample size	Sample size was chosen based on availability of plasma where the SARS-CoV-2 variant eliciting the immune response was sequenced (plasma samples from the first South African infection wave) or availability of plasma (second South African infection wave).
Data exclusions	We have predetermined that no plasma which does not neutralize the matched variant (ie, first South African wave variant for first wave plasma, 501Y.V2 virus for second wave plasma) will not be used. On this basis, we excluded 1 first wave plasma and 2 second wave plasma samples.
Replication	All data was replicated in multiple experiments and for multiple plasma donors. The exception is plasma from a participant elicited by virus with the E484K mutation only, as we only identified one such participant. Nevertheless, we included the E484K data as speculative, with the hypothesis that this mutation leads to an effective cross-neutralizing antibody response to be confirmed or rejected by data from other groups. Other plasma donors were grouped into two groups: 1) Those infected in the first South African SARS-CoV-2 infection wave (no 501Y.V2 defining mutations and infected before November 1, 2020). There were samples from n=14 different participants for this group; 2) those infected in the second South African SARS-CoV-2 infection wave (501Y.V2 defining mutations and infected after November 1, 2020). There were samples from n=6 different participants for this group. For plasma from participants 039-13-0037, 039-13-0038, 039-13-0060, 039-13-0103, 039-02-0030, 039-02-0031, 039-02-0033, we performed 4 independent neutralization experiments. For all other participants, we performed 3 independent experiments. All attempts at replication were successful.
Randomization	Participants allocated based on whether they were infected with the 501Y.V2 or earlier variants circulating in South Africa.
Blinding	Blinding was not possible as participant plasma from the second South African infection wave was received midway during the study after some plasma from the first South African wave was already tested.

Reporting for specific materials, systems and methods

We require information from authors about some types of materials, experimental systems and methods used in many studies. Here, indicate whether each material, system or method listed is relevant to your study. If you are not sure if a list item applies to your research, read the appropriate section before selecting a response.

Materials & experimental systems

n/a	Involved in the study
☐	☒ Antibodies
☐	☒ Eukaryotic cell lines
☒	☐ Palaeontology
☒	☐ Animals and other organisms
☐	☒ Human research participants
☐	☒ Clinical data

Methods

n/a	Involved in the study
☒	☐ ChIP-seq
☒	☐ Flow cytometry
☒	☐ MRI-based neuroimaging

Antibodies

Antibodies used	Genscript A02051 as positive control for neutralization. GenScript A02058 for staining of infected cells. Abcam ab205718 Goat anti-Rabbit HRP conjugated antibody was the secondary antibody for HRP based visualization of infection foci. The anti-spike RBD CR3022 antibody (A gift from Aaron Schmidt, Ragon Institute) was used in ELISA.
Validation	A02051 was validated by titration. A02058 was validated by positive and negative infection controls. More information can be found at: https://www.genscript.com/antibody/A02051-MonoRab_SARS_CoV_2_Neutralizing_Antibody_BS_R2B2_mAb_Rabbit.html?position_no=1&sensors=search%20product%20box. ab205718 validation can be found at https://www.abcam.com/goat-rabbit-igg-hl-hrp-ab205718.html. CR3022 binding to spike RBD is described in https://www.abcam.com/sars-cov-2-spike-glycoprotein-s1-antibody-cr3022-ab273073.html.

Eukaryotic cell lines

Policy information about cell lines

Cell line source(s)	H1299: ATCC (CRL-5803). HEK-293: ATCC (CRL-1573). Vero E6: Cellonex (http://cellonex.azurewebsites.net/) expansion of ATCC CRL-1586.
Authentication	None of the cell lines were authenticated
Mycoplasma contamination	Confirmed mycoplasma negative
Commonly misidentified lines (See ICLAC register)	None

Human research participants

Policy information about studies involving human research participants

Population characteristics	The study population for plasma donors was adults hospitalized with PCR-confirmed COVID-19, regardless of age, severity of disease, and HIV status, which are recorded in Table S1. Time from symptom onset or initial diagnosis (if asymptomatic) and blood draw from plasma was approximately 1 month.
Recruitment	Nasopharyngeal/oropharyngeal swab samples and plasma samples were obtained from 20 hospitalized adults with PCR confirmed SARS-CoV-2 infection enrolled in a prospective cohort study. Potential source of bias are: 1) Bias against severe cases of COVID-19 disease due to difficulty in recruitment due to challenges filing out questionnaire while in poor clinical state; 2) bias to increased enrollment of females because of higher linkage to care of this group in the South African context. Bias 1 is not likely to influence results since severe disease is not representative of the population. 40% male participants were recruited despite bias 2 and these were in similar frequencies across the two groups, so this bias is not expected to affect results.
Ethics oversight	Combined sampling of COVID-19 participants through blood draw and swab was approved by the Biomedical Research Ethics Committee (BREC) at the University of KwaZulu-Natal (reference BREC/00001275/2020). The 501Y.V2 variant was obtained from residual swab samples used for diagnostic testing by the National Health Laboratory Service (BREC approval reference BREC/00001510/2020).

Note that full information on the approval of the study protocol must also be provided in the manuscript.

Clinical data

Policy information about clinical studies

All manuscripts should comply with the ICMJE guidelines for publication of clinical research and a completed CONSORT checklist must be included with all submissions.

Clinical trial registration	N/A, observational prospective cohort study
Study protocol	Study protocol is available upon request.
Data collection	Patients hospitalized in three Durban facilities (Inkosi Albert Luthuli Central Hospital, King Edward Hospital, and Clairwood Hospital) with confirmed SARS-CoV-2 infection by qPCR were eligible for enrollment. Clinical data including symptoms, requirement for supplemental oxygen, BMI, and other parameters were collected at enrollment and at weekly intervals thereafter. Accredited tests were performed with a service laboratory to determine HIV status and HIV viral load.
Outcomes	N/A, non-interventional.